https://doi.org/10.18524/1810-4215.2025.38.343162

USING CLUSTER CARTOGRAPHY 2D+ FOR DETECTING SUBSTRUCTURES IN THE 3D GALAXY CLUSTERS

E. A. Panko[1], S. I. Yemelianov[2], D. O. Lavreniuk[1]

[1] Odesa I. I. Mechnikov National University, Odesa, Ukraine, *panko.elena@gmail.com*
[2] Mykolaiv National Agrarian University, Mykolaiv, Ukraine, *sviatoslavem@gmail.com*

ABSTRACT. In our detailed study of the inner structure of PF galaxy clusters, we found different kinds of substructures in these objects. Most of the detected substructures are quite common. In addition to the classical filamentary features described by Rood and coauthors' papers, we include complex cross-shaped substructures and short dense chains of galaxies as regular. We suppose that regular substructures are connected with the Large-Scale Structure of the Universe elements, which form the parent cluster node. Our previous studies were based on the list of galaxies of the Muenster Red Sky Survey, which has no redshifts. It allowed us to study only the 2D distribution of galaxies inside the cluster. Modern data, such as the Sloan Digital Sky Survey, the VIMOS Public Extragalactic Redshift Survey, the Euclid Wide Survey, and others, give us the opportunity for 3D studies of these objects.

We improved the base online version of the "Cluster Cartography 2D" tool (*https://clustercartography.github.io/*) into the "Cluster Cartography 2D+" tool. It allows to apply the algorithms developed for 2D version to the detection of regular substructures on a statistically significant level for the 3D distribution of galaxies in the rectangular projections. We tested this opportunity on artificial galaxy clusters with different kinds of substructures. We have shown that using 2D projections allows us to detect the 3D regular substructures, and to restore their real shapes and directions.

Keywords: Universe, LSC: galaxy clusters: morphology: inner structure, substructures; data analysis.

АНОТАЦІЯ. В наших попередніх роботах, що присвячені детальному дослідженню внутрішньої будови скупчень галактик каталогу PF, були виявлені різні види підструктур у цих об'єктах. Більшість виявлених підструктур зустрічаються досить часто. На додаток до класичних філаментарних особливостей, що були описані ще у статтях Руда та співавторів, ми включаємо до регулярних підструктур складні хрестоподібні утворення та короткі щільні ланцюжки галактик. Таки підструктури, скоріше за все, пов'язані з елементами Великомасштабної Структури Всесвіту, що формють вузол, в якому виникає скупчення галактик. Наше дослідження базувалося на списку галактик Мюнстерського огляду червоного неба (Muenster Red Sky Survey), який дозволяє нам вивчати лише 2D розподіл галактик всередині скупчення. Сучасні дані, такі як Sloan Digital Sky Survey, VIMOS Public Extragalactic Redshift Survey, Euclid Wide Survey та інші, дають можливість 3D досліджень для цих об'єктів.

Ми вдосконалили базову онлайн-версію програми Cluster Cartography (*https://clustercartography.github.io*) до 2D рівня Cluster Cartography 2D+. Це дозволяє застосовувати алгоритми, які було розроблено та протестовано у 2D версії, до виявлення регулярних субструктур на статистично значущому рівні для 3D розподілу галактик у прямокутних проекціях. Ми перевірили ці можливості на штучних скупченнях галактик з різними видами субструктур. Ми показали, що використання 2D проекцій дозволяє нам виявляти 3D регулярні підструктури та відновлювати їх реальні форми та орієнтації.

Ключові слова: Всесвіт, Великомасштабна структура: скупчення галактик: морфологія: внутрішня будова, субструктури; аналіз даних.

1. Introduction

The elements of the Large Scale Structure of the Universe (LSS) evolve in interaction with its surroundings. The co-evolution of LSS elements was established in the base theoretical works like Silk (1968), Peebles (1969), Peebles & Yu (1970), Zeldovich (1970), and most recently. The initial fluctuations of the density and Hubble flow produce the different variants

of expansion/contraction: 3D contraction gives spherical or ellipsoidal structures, 2D leads to filaments, and the walls are formed due to 1D contraction. According to modern scenarios, the evolution of the elements of LSS occurs in interaction with its surroundings. This co-evolution of LSS elements was established in the base theoretical works like Silk (1968), Peebles (1969), Peebles & Yu (1970), Zeldovich (1970), and most recently. The initial fluctuations of the density and Hubble flow produce the different variants of expansion/contraction: 3D contraction gives spherical or ellipsoidal structures, 2D leads to filaments, and the walls are formed due to 1D contraction. The numerical simulations from the first (Klypin & Shandarin, 1983) to the latest (Springel et al., 2005, Vogelsberger et al., 2014, Artale et al., 2017, Cui et al., 2018, Tomoaki et al., 2021) showed that the multi-speed expansion leads to the arising Cosmic web nodes in the crossing filaments and walls, and the largest LSS elements, such as galaxy clusters or superclusters, occur in the nodes of the cosmic web. It corresponds to the results of the observations (Wen et al., 2009, Dietrich et al., 2012, Parekh et al., 2020). Tracing the cosmic web in the densest nodes allows us to detail the constraints of the cosmological models. The number of filaments connected to a given node is attributed as the node connectivity or multiplicity. Theory and simulations show that connectivity and multiplicity can be expected to increase with node mass or environmental density (Aragón-Calvo et al., 2010, Codis et al., 2018, Gouin et al., 2021; Kraljic et al., 2022, Malavasi et al., 2023). In observations, connectivity multiplicity in relation to its mass, dynamical status, and galaxy population was explored at galaxy cluster scales in Sarron et al. (2019), Darragh Ford et al., (2019), Lee et al. (2019). Probably, the node's connectivity at galaxy cluster scales must manifest inside the cluster as corresponding substructures at the same stage of evolution according to Struble & Rood (1987).

Our previous research was directed to the study of substructures in galaxy clusters in fields with different densities, from the richest regions (Panko et al., 2021) to isolated galaxy clusters (Panko et al., 2022). In all cases, we detected the different kinds of regular substructures, such as linear ones from wide bands to thin filaments, crosses and semi-crosses, and short dense curve stripes in the 2D distribution of galaxies for PF galaxy clusters (Panko & Flin, 2006). Our approach was described in Panko (2025), and Yemelyanov & Panko (2021) papers. We detected substructures in the clusters, which are probably footprints of the filaments connected to the parent cluster node.

"Cluster Cartography 2D" tool, CC 2D further, https://clustercartography.github.io/ is used to study substructures on galaxy clusters for 2D input data. The improved "Cluster Cartography 2D+" tool, on the same web page, allows us to detect substructures in 3D data. In the paper, we discussed the perspectives of the improved tool for the 3D study of galaxy clusters, using a simulated distribution of galaxies in the cluster. In the future, the CC 2D+ tool can be used for modern data of the Sloan Digital Sky Survey (SDSS, York et al., 2000),, the VIMOS Public Extragalactic Redshift Survey (VIPERS, Scodeggio et al., 2018), or the Euclid Wide Survey (EWS, Euclid Collaboration: Scaramella et al., 2022).

2. "Cluster Cartography 2D+"

Web version of CC 2D tool contains functions for processing data, calculating statistics, and plotting maps, histograms, and graphics, which are built using different parameters, such as the radii and widths of the rings in determining the degree of the concentration to the center, the widths of the bands in determining of the degree of the concentration in the linear substructures, the presence of the Binggeli effect (Binggeli, 1982) both for all galaxies and separated substructures, etc. (Yemelyanov & Panko, 2021). We can search for the position of the greatest density of galaxies in the cluster field, detect the regular linear and cross-type substructures, study the rope of the brightest galaxies, and analyze the shape of the members of the cluster based on the algorithms described in Panko (2025) paper. We can also create a list of galaxies forming the regular substructures.

The difference in the CC 2D+ input file is the 3rd coordinate placed in the last column. All the capabilities of the CC 2D+ version was retained and can be used for various projections of 3D data. The RA and Dec data correspond to the X and Y coordinate axes, and the distance or redshift z corresponds to the Z axis. If we have no distance or need to analyze the 2D data, the last column is not considered.

In the CC 2D+, the RA and Dec coordinates of galaxies are shown as the projection of one from our test cluster onto the celestial sphere (Fig. 1*a*). The 2D+ tool allows us to create the 3D color map of the cluster, where the color of the symbol illustrates the galaxy distance from the cluster center. CC 2D+ gives the possibility to rotate the cluster and to create cluster maps in the other projections XZ and YZ, where Z is the distance/redshift of the galaxy (Fig. 1*b, c*). Thus, we can study the 3D distribution of galaxies in three rectangular projections: RA and Dec, RA and z, Dec. and z. The ability to rotate the cluster to an arbitrary angle also allows us to find the best orientation for visibility of the substructure. It is illustrated in Fig. 2. The initial view of the cluster is shown in Fig. 2*a*, while the turned cluster in Fig. 2*b* shows all linear elements of the compound cross.

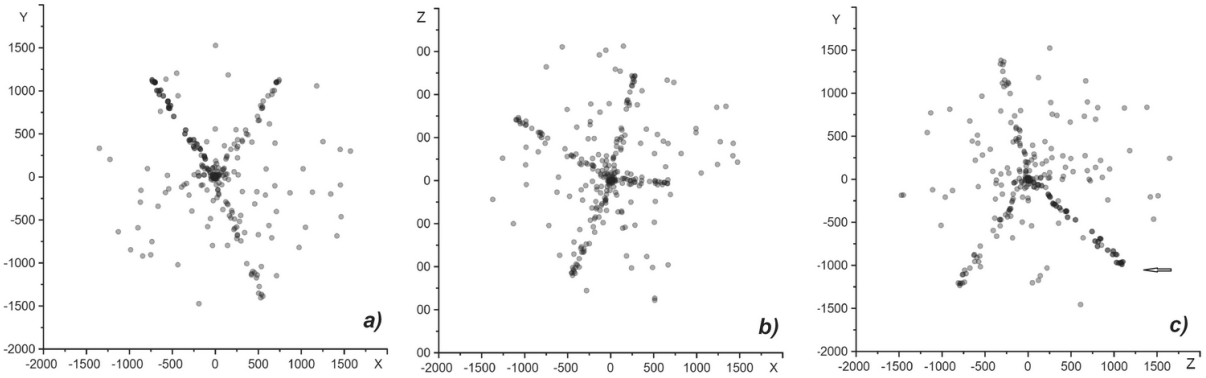

Figure 1: Artificial open cluster with 3D compound cross-type substructure in the different projections: *a*) for RA and Dec. axes, *b*) for RA and *z* axes, and *c*)for Dec. and *z* axes, arrow points to 2 stripes of the cross combined in Dec− *z* projection

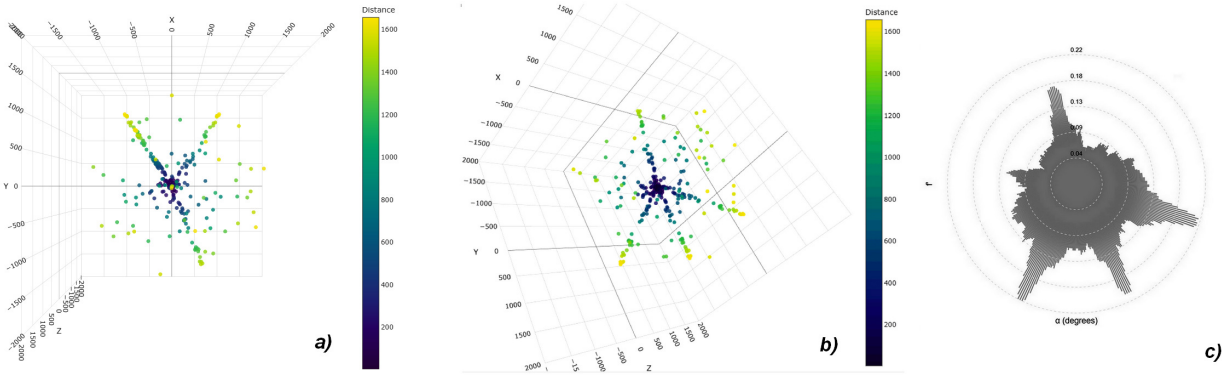

Figure 2: The 3D map of the artificial cluster with compound cross: *a*) initial view, *b*) turned map, all components of the compound cross are clearly seen, *c*) radial LightHouseBeam diagram fir the turned map

3. 3D substructures search discussion

For testing the CC 2D+ tool, we create a set of artificial galaxy clusters with different morphologies and substructure' types. We constructed the next types of distribution of galaxies:

- the cluster open type as a base element for the next steps;
- the cluster with the spherical or ellipsoidal core;
- the open cluster with the wall;
- the open cluster with the single filament;
- the open cluster having a compound 3D substructure cross-type.

All simulated features were constructed based on an open cluster with additional elements. The distributions of the galaxies in a thin wall or filaments were constructed using the Box - Miller transformation.

Obviously, the degree of concentration of galaxies toward the cluster center does not depend on the projection. Nevertheless, such clusters we must consider in the three projections for the estimation of the real core shape and orientation.

The filament inside the cluster looks like linear substructure in all projections, except for the case of special orientation: when the filament directs along the line of sight, it will be seen as a concentration towards the cluster center, and we obtain the false morphological classification as "Concentrated cluster". If the angle between the linear substructure and the line of sight is small, we detect it as a dense short chain. They are rare special cases. However, we must take into account these.

Another rare special case is the wall-type substructure, which is seen as a filament. But, in some projections, we can lose such a substructure in the background of other cluster members. The 2D+ tool allows us to rotate the 3D cluster map. It gives the possibility

of confident detection for all filaments and walls with visual control.

The last test artificial cluster with the compound cross connecting 4 different filaments, is shown in Fig. 1 in all projections. The some cross elements can be lost in projections, as in Fig 1*c*. The initial 3D color map of the test cluster is shown in Fig. 2*a*. It's like to RA–Dec. projection map (Fig. 1*a*). The optimal view of the substructure is shown in Fig. 2*b*, and the corresponding radial LightHouseBeam diagram is present in Fig. 2*c*. The diagram was created on the 2D projection of the rotated cluster. This diagram is the visualization of LightHouseBeam analysis, which shows all linear elements of the compound cross.

The reliability of the real substructures identification is confirmed by both the observed distribution of bright galaxies in the cluster and the alignment of galaxies relative to substructures in accordance with the work of Joachimi et al. (2015). For the PF clusters we have the 2D position and orientations for galaxies from Muenster Red sky Survey (Ungrue at al., 2003) Unfortunately, in 3D we have no space alignment of galaxies, even if we have the distances. So, in the 3D case, we can confirm the reliability of the substructure only by the brightest galaxies' positions.

The observational data for our further research can be selected in the NASA/IPAC Extragalactic Database (https://www.ipac.caltech.edu/project/ned, https://ned.ipac.caltech.edu/), where some PF Galaxy Clusters (Panko & Flin, 2006) are present too.

4. Conclusion

We created the "Cluster Cartography 2D+" tool, which allows the detection of regular substructures in 3D data for galaxy clusters. All types of substructures, such as planes, filaments, and complex crosses, can be detected in three projections: RA and Dec., RA and z, and Dec. and z, using corresponding well-tested algorithms. In the CC 2D+ tool, we can also create 3D maps and turn them for an arbitrary angle for the best visibility of the substructure. The CC 2D+ tool is advisable for estimating the central core shape and orientation, too. We plan to create the Spherical Density Chart (3D analog of the Polar Density Chart in LightHouseBeam analysis) and use our tool to study the galaxy clusters in modern 3D data.

Acknowledgments. The authors express their sincere gratitude to the independent referee, Dr. Dominique Proust, for helpful comments on our paper.

This research has made use of NASA's Astrophysics Data System. This research has made use of the NASA/IPAC Extragalactic Database, which is funded by the National Aeronautics and Space Administration and operated by the California Institute of Technology.

References

Aragón-Calvo M. A., van de Weygaert R. & Jones B. J. T.: 2010, *MNRAS*, **408**, 2163.
Binggeli B.: 1982, *A&A*, **107**, 338.
Codis S., Pogosyan D., & Pichon C.: 2018, *MNRAS*, **479**, 973.
Cui W., Knebe A., Yepes G., et al.: 2018, *MNRAS*, **473**, 68.
Darragh Ford E., Laigle C., Gozaliasl G., et al.: 2019, *MNRAS*, **489**, 5695.
Dietrich J. P., Werner N., Clowe D., et al.: 2012, *Nature*, **487**, 202.
Gouin C., Bonnaire T., & Aghanim N.: 2021, *A&A*, **651**, A56.
Joachimi B., Cacciato M., Kitching T. D., et al.: 2015, *Space Sci. Rev.*, **193**, 1.
Klypin A.A. & Shandarin S.F.: 1983, *MNRAS*, **204**, 891.
Kraljic K., Laigle C., Pichon C., et al.: 2022, *MNRAS*, **514**, 1359.
Lee S.-K., Im M., Hyun M., et al.: 2019, *MNRAS*, **490**, 135.
Malavasi N., Sorce J. G., Dolag K., & Aghanim N.: 2023, *A&A*, **675**, A76.
Panko E. A.: 2025, *Universe*, **11**, 7, id.238.
Panko E. A. & Flin P.: 2006, *J. Astron. Data*, **12**, 1.
Panko E., Yemelianov S., Korshunov V., et al.: 2021, *Astron. Rep.*, **65**, 1002.
Panko E. A., Yemelianov S., Sirginava A., & Pysarevskyi Z.: 2022, *ComBAO*, **69**, 256.
Parekh V., Lagana T. F., Tho K., et al.: 2020, *MNRAS*, **491**, 2605.
Peebles P.: 1969, *AJ*, **155**, 393.
Peebles P. J. E. & Yu J. T.: 1970, *ApJ*, **162**, 815.
Sarron F., Adami C., Durret F., & Laigle, C.: 2019, *A&A*, **632**, A49.
Scaramella R., Amiaux J., Mellier Y.,at al.: 2022, *A&A*, **662**, A112.
Scodeggio M., Guzzo L., Garilli B., et al.: 2018, *A&A*, **609**, A84.
Silk J.: 1968, *ApJ*, **151**, 459.
Springel V., White S. D., Jenkins A., et al.: 2005, *Nature*, **435**, 629.
Struble M. F. & Rood H. J.: 1987, *ApJSS*, **63**, 555.
Tomoaki A. A., Francisco P., Klypin A. A., et al.: 2021, *MNRAS*, **506**, 4210.
Ungrue R., Seitter W. C., Duerbeck H. W.: 2003, *J. Astron. Data*, **9**, 1.
Vogelsberger M., Genel S., Springel V., et al.: 2014, *MNRAS*, **444**, 1518.
Wen Z.L., Han J.L. & Liu A.C.: 2009, *ApJSS*, **183**, 197.
Yemelyanov S. I. & Panko E. A.: 2021, *OAP*, **34**, 35.
York D. G., Adelman J., Anderson John E. J., et al.: 2000, *AJ*, **120**, 1579.
Zeldovich Y. B.: 1970, *A&A*, **5**, 84.
Zeldovich Y., Einasto J. & Shandarin S.: 1982, *Nature*, **300**, 407.